JACC: CARDIOVASCULAR IMAGING VOL. 1, NO. 1, 2008

ISSN 1936-878X/08/$34.00
PUBLISHED BY ELSEVIER DOI:10.1016/j.jcmg.2007.10.006

Disparate Patterns of Left Ventricular Mechanics Differentiate Constrictive Pericarditis From Restrictive Cardiomyopathy

Partho P. Sengupta, MD,* Vijay K. Krishnamoorthy, MD,† Walter P. Abhayaratna, MBBS,† Josef Korinek, MD,† Marek Belohlavek, MD, PHD,* Thoralf M. Sundt, III, MD,† Krishnaswamy Chandrasekaran, MD,* Farouk Mookadam, MD,* James B. Seward, MD,† A. Jamil Tajik, MD,* Bijoy K. Khandheria, MD*

Scottsdale, Arizona; and Rochester, Minnesota

OBJECTIVES The purpose of this study was to compare the longitudinal, circumferential, and radial mechanics of the left ventricle (LV) in patients with constrictive pericarditis (CP) and restrictive cardiomyopathy (RCM).

BACKGROUND Diastolic dysfunction in CP is related to epicardial tethering and pericardial constraint, whereas in RCM it is predominantly characterized by subendocardial dysfunction. Assessment of variations in longitudinal and circumferential deformation of LV might be useful to distinguish these 2 conditions.

METHODS Longitudinal, radial, and circumferential mechanics of the LV were quantified by 2-dimensional speckle tracking of B-mode cardiac ultrasound images in 26 patients with CP, 19 patients with RCM, and 21 control subjects.

RESULTS In comparison with control subjects, patients with CP had significantly reduced circumferential strain (base; $-16 \pm 6\%$ vs. $-9 \pm 6\%$; $p < 0.016$), torsion ($3 \pm 1°/cm$ vs. $1 \pm 1°/cm$; $p < 0.016$), and early diastolic apical untwisting velocities (E_r; $116 \pm 62°/s$ vs. $-36 \pm 50°/s$; $p < 0.016$), whereas longitudinal strains, displacement, and early diastolic velocities at the LV base (E_m) were similar to control subjects. In contrast, patients with RCM showed significantly reduced longitudinal displacement (base; 14.7 ± 2.5 cm vs. 9.8 ± 2.8 cm; $p < 0.016$) and E_m (-8.7 ± 1.3 cm/s vs. -4.4 ± 1.1 cm/s; $p < 0.016$), whereas circumferential strain and E_r were similar to those of control subjects. For differentiation of CP from RCM, the area under the curve was significantly higher for E_m in comparison with E_r (0.97 vs. 0.76, respectively; $p = 0.01$). After pericardiectomy, there was a significant decrease in longitudinal early diastolic LV basal myocardial velocities (7.4 cm/s vs. 6.8 cm/s; $p = 0.023$). Circumferential strain, torsion, and E_r, however, remained unchanged.

CONCLUSIONS Deformation of the LV is constrained in the circumferential direction in CP and in the longitudinal direction in RCM. Subsequent early diastolic recoil of LV is also attenuated in each of the 2 directions, respectively, uniquely differentiating the abnormal diastolic restoration mechanics of the LV seen in CP and RCM. (J Am Coll Cardiol Img 2008;1:29–38) © 2008 by the American College of Cardiology Foundation

From the *Division of Cardiovascular Diseases, Mayo Clinic Arizona, Scottsdale, Arizona; and the †Division of Cardiovascular Diseases, Mayo Clinic, Rochester, Minnesota. This work was supported by a Grant-in-Aid from the American Society of Echocardiography (Dr. Sengupta).

Manuscript received September 5, 2007; revised manuscript received October 9, 2007, accepted October 18, 2007.

JACC: CARDIOVASCULAR IMAGING, VOL. 1, NO. 1, 2008
JANUARY 2008:29–38

The helical orientation of the myofibers in the left ventricle (LV) is the structural basis of the wringing motion of the LV in systole, where the apex moves counterclockwise and the base moves clockwise (1). Rotation of the apex with respect to the base, counterclockwise in systole, is referred to as twist or torsion (twist normalized to length) and results in storage of potential energy. This energy is used for LV diastolic recoil and contributes to ventricular suction and early diastolic filling (1,2).

During early diastolic recoil and untwisting, the magnitude of circumferential and longitudinal expansion of the LV is modulated by stiffness of pericardial layers (3,4). At lower LV volumes, the pericardium expands, but after a certain LV volume, it stiffens and resists further circumferential expansion (3,4). Loss of normal compliance of pericardial layers might alter the pattern of circumferential and longitudinal diastolic recoil. For example, it has been previously suggested that LV expansion and filling in constrictive pericarditis (CP) might be limited in the circumferential rather than the longitudinal direction (5). Moreover, scarring and inflammation from pericardial layers might extend into the myocardial wall in CP (6–8), which might further attenuate the circumferential recoil of the LV in CP. The relationship between LV circumferential deformation, torsion, and subsequent early diastolic recoil in CP, however, has not been sufficiently elucidated.

ABBREVIATIONS AND ACRONYMS

2D = 2-dimensional
CP = constrictive pericarditis
LV = left ventricle/ventricular
RCM = restrictive cardiomyopathy

The recent introduction of 2-dimensional (2D) speckle tracking of B-mode cardiac ultrasound images has facilitated rapid and accurate measurement of longitudinal and circumferential myocardial deformation including torsion (9). Preliminary observations suggest the existence of an inverse relationship between longitudinal LV dynamics and twist deformation (10). Myocardial diseases primarily manifesting with endocardial dysfunction show abnormal longitudinal LV motion while relatively sparing of LV twist (10,11). It is not known, however, whether relative differences between long axis motion and LV twist would be useful to distinguish the mechanism of diastolic dysfunction in conditions such as CP and restrictive cardiomyopathy (RCM). Therefore, the goal of this study was to compare and contrast the relative differences between longitudinal, circumferential, and torsional mechanics of the LV in patients with CP and RCM.

METHODS

The study was approved by the Mayo Foundation Institutional Review Board. Between July 2005 and January 2007, we prospectively identified 37 consecutive patients with CP who were scheduled for pericardiectomy and 22 patients with heart failure who were diagnosed with RCM with transthoracic echocardiography. Seven patients with CP were excluded because of suboptimal 2D-echocardiography image quality. Of the remaining patients, 26 with CP and 19 with RCM consented to participation in the study. We also recruited 21 control subjects without overt cardiovascular disease or echocardiographic evidence of LV dysfunction or significant valvular heart disease. Attempts were made to match control subjects to CP patients with regard to age and gender.

All patients with CP had clinical and echocardiographic evidence of increased right-sided filling pressures. Respiratory variations in Doppler transmitral early diastolic flow velocity (>25%) were seen in 16 (62%) patients. Additional tests for preoperative assessment of CP included computerized tomography in 15 (58%), cardiac magnetic resonance imaging in 4 (15%), coronary angiography in 18 (69%), and assessment of cardiac hemodynamic status by cardiac catheterization in 11 (42%) patients. During surgery, in all CP patients, left- and right-sided filling pressures improved immediately with the removal of pericardium. The underlying cause of CP was previous cardiac surgery in 5 (19%), radiotherapy in 8 (31%), viral pericarditis in 5 (19%), and idiopathic in 8 (31%) patients.

Restrictive cardiomyopathy was defined as myocardial disease that was characterized by restrictive physiology demonstrated by Doppler transmitral diastolic flow velocity, reduced diastolic LV volumes, and LV ejection fraction >45%. The underlying etiology of RCM was cardiac amyloidosis in 15 (79%) and idiopathic RCM in 4 (21%) patients. All patients with cardiac amyloidosis had biopsy-proven systemic amyloidosis.

Standard B-mode and Doppler echocardiography. Studies were performed at baseline (Vivid 7, GE Healthcare, Milwaukee, Wisconsin) and repeated just before hospital discharge in patients with CP who underwent pericardiectomy as per standard guidelines (12). Pulsed-wave Doppler transmitral velocity and hepatic venous flow velocities were recorded simultaneously with respiratory tracing. Septal mitral annulus velocities were measured in the apical 4-chamber view. All measurements were averaged over 3 cardiac cycles.

2D strain echocardiography. Parasternal short-axis (apical, mid, and basal segments) and apical 4-chamber views of the LV were recorded at end-expiration (60 to 110 frames/s) and probe frequency (range 1.7 to 2.0 MHz). To standardize short-axis image planes among the individuals, we identified the basal LV segment at the level of the mitral valve leaflet tips and the apical segment at the level just proximal to LV luminal obliteration at the end-systolic period. To obtain reliable LV 2D strain and rotation values, 3 consecutive heartbeats were digitally saved in cineloop format for later offline analysis with commercially available software (EchoPac 6.0.1 for PC, GE Healthcare). This software has been previously validated and allows accurate tracking acoustical markers (speckle patterns) on sequential echocardiographic images with correlation criteria and sum of absolute differences (13,14). The width for the region of interest was optimized to include at least 50% of the LV wall from the endocardial side. The software then automatically captured a multitude of local myocardial acoustical markers and tracked their displacement through a cine loop of frames. Longitudinal, radial, and circumferential strains were computed from the resulting 2D displacement fields.

Parameters defining LV mechanics were averaged from 6 segments in short-axis views and from lateral and septal wall segments in apical 4-chamber views. The LV rotations in either the basal or apical short-axis planes were expressed as average angular displacements of 6 myocardial segments along the central axis. By convention, counterclockwise LV rotation as viewed from the apex is expressed as a positive value and clockwise LV rotation as a negative one. After procurement of the LV rotation at the 2 short-axis levels, net LV twist was calculated as the net difference between LV peak rotation angles obtained from basal (clockwise) and apical (counterclockwise) short-axis planes. The LV torsion was calculated as the net LV twist normalized with respect to ventricular diastolic longitudinal length between the LV apex and the mitral plane (i.e., LV torsion [°/cm] = [apical LV rotation − basal LV rotation]/LV diastolic longitudinal length). We also measured the peak twist rates during ejection and untwisting rates in early and late diastole.

Assessment of the LV longitudinal strain or rotation was regarded as suboptimal when either: 1) speckle tracking could not be obtained for at least 4 of the 6 myocardial segments in apical 4-chamber or short-axis views; or 2) a theoretically unaccept-

Table 1. Patient Characteristics

	Control Subjects (n = 21)	CP (n = 26)	RCM (n = 19)	p Value*
Age, yrs	45 (17)	56 (13)	62 (10)	0.13†
Women, n (%)	11 (52)	10 (38)	9 (47)	0.08
Body surface area, m^2	1.90 (0.17)	1.94 (0.25)	1.82 (0.23)	0.15
Systolic blood pressure, mm Hg	124 (18)	107 (14)	107 (15)	0.93†
Diastolic blood pressure, mm Hg	73 (13)	68 (8)	67 (11)	0.63
Heart rate, beats/min	62 (11)	77 (19)	78 (10)	0.75†
LV septum, mm	10 (1)	9 (1)	13 (2)	<0.001
LV posterior wall, mm	10 (1)	9 (1)	13 (2)	<0.001†
LV end-diastolic dimension, mm	41 (5)	43 (6)	42 (5)	0.32
LV end-systolic dimension, mm	26 (5)	29 (4)	27 (5)	0.06†
LVEF, %	66 (4)	57 (8)	61 (7)	0.08†
LA volume indexed, ml/m^2	26 (8)	37 (13)	45 (15)	0.04†
E velocity, m/s	0.69 (0.16)	0.91 (0.43)	0.98 (0.48)	0.50†
A velocity, m/s	0.46 (0.13)	0.46 (0.13)	0.70 (0.28)	0.01
E/A ratio	1.7 (0.9)	2.0 (1.0)	1.5 (0.5)	0.06
Deceleration time, ms	218 (46)	150 (35)	189 (61)	0.01†
Medial annulus E_a velocity, m/s	0.14 (0.05)	11.2 (4.4)	4.6 (1.1)	0.005†
E/E_a	6 (2)	12 (9)	22 (11)	<0.001†
RA pressure, mm Hg	—	13 (6)	9 (5)	0.03
RV systolic pressure, mm Hg	—	40 (11)	38 (11)	0.24

*Constrictive pericarditis (CP) versus restrictive cardiomyopathy (RCM) groups; †CP versus control subjects, $p < 0.05$.
A = peak late diastolic transmitral flow velocity; E = peak early diastolic transmitral flow velocity; E_a = early diastolic mitral annular velocity; EF = ejection fraction; LA = left atrium; LV = left ventricle; RA = right atrium; RV = right ventricle.

Table 2. Characterization of LV Longitudinal, Circumferential, and Radial Mechanics

	Control Subjects (n = 21)	CP (n = 26)	RCM (n = 19)	p Value
Longitudinal				
Displacement, LV base, cm	14.7 (2.5)	12.1 (2.6)*†	9.8 (2.8)‡	<0.001
Velocity, LV base, cm/s				
Peak S	6.4 (1.2)	5.4 (1.6)*	5.1 (1.7)‡	0.007
Peak E	−8.7 (1.3)	−7.6 (2.0)†	−4.4 (1.1)‡	<0.001
Peak A	−6.4 (1.6)	−4.4 (2.2)*	−4.6 (2.8)	0.02
Strain, %				
Apex	−20 (4)	−15 (4)*	−13 (5)‡	<0.001
Mid	−18 (3)	−17 (3)†	−13 (4)‡	<0.001
Base	−14 (6)	−15 (4)†	−11 (4)	0.02
Circumferential				
Strain, %				
Apex	−27 (10)	−18 (6)*†	−26 (9)	<0.001
Mid	−19 (6)	−14 (6)*†	−22 (7)	0.001
Base	−16 (6)	−9 (6)*†	−17 (7)	0.001
Radial				
Displacement, cm				
Apex	4.4 (1.5)	3.1 (1.4)*†	4.3 (1.4)	0.005
Mid	4.4 (1.2)	3.0 (1.4)*†	4.1 (1.8)	0.004
Base	2.7 (1.9)	1.5 (1.4)*†	3.0 (1.6)	0.01
Strain, %				
Apex	13 (10)	11 (8)	15 (11)	0.51
Mid	40 (19)	27 (16)	28 (14)	0.04
Base	44 (22)	22 (15)*	24 (11)‡	0.003

*Constrictive pericarditis (CP) versus control subjects, $p < 0.016$; †CP versus restrictive cardiomyopathy (RCM) patients, $p < 0.01$; ‡RCM versus control subjects, $p < 0.016$.
A = late diastole; E = early diastole; LV = left ventricular; S = ejection.

able value or values were obtained. Offline analyses were independently performed by 2 observers who were not involved in the image acquisition and had no knowledge of other echocardiographic measures of LV function.

Statistical analysis. Descriptive data were summarized as frequency percentages for categorical variables or mean ± SD for continuous variables. Characteristics of the CP, RCM, and control groups were compared with the Kruskal-Wallis test, and paired comparisons were performed with the Student *t* test with adjustment for multiple comparisons through Bonferroni correction. The interrelationships between the 2D strain, twist, and Doppler hemodynamic variables were assessed with Spearman's correlation. The overall performances of various echocardiographic variables for discriminating CP from RCM were quantified with receiver-operating characteristic analysis and were compared with the method of DeLong. Changes in the LV mechanics after pericardiectomy were assessed with a paired *t* test. Statistical significance was defined as a 2-tailed $p < 0.05$.

RESULTS

Baseline clinical and echocardiographic characteristics of the control group and patients with CP and RCM are displayed in Table 1. The LV internal dimensions, ejection fraction, left atrial volumes, and early/late diastolic transmitral flow velocity ratios were similar in both groups. Patients with RCM had significantly higher LV wall thickness ($p < 0.001$), longer deceleration time ($p = 0.01$), higher peak atrial filling velocity ($p = 0.01$), and a lower ratio of early diastolic mitral flow velocity to medial annular lengthening velocity ($p < 0.001$).

Longitudinal mechanics of LV. Longitudinal displacement of the LV base in systole was reduced in CP and RCM when compared with control subjects (Table 2). However, longitudinal early diastolic mitral annular velocity obtained by pulsed wave tissue Doppler (Table 1) and early diastolic lengthening velocities obtained from LV basal segments (Table 2) were significantly higher in CP when compared with RCM ($p < 0.05$ and $p < 0.001$, respectively). Longitudinal shortening strain recorded from the LV basal segment

was significantly higher for control subjects and CP in comparison with RCM ($p < 0.001$). In contrast, the longitudinal shortening strains from the LV apex were reduced equally in CP and RCM when compared with control subjects ($p < 0.001$). Longitudinal early diastolic velocities obtained from the LV base were significantly lower in patients with CP with secondary causes such as surgery, mediastinal radiation, and pericarditis in comparison with CP of idiopathic origin (9.2 cm/s vs. 6.8 cm/s, $p = 0.002$). There was no difference between the idiopathic and secondary CP subgroups, however, for the magnitude of longitudinal strain.

After pericardiectomy, there was a significant decrease in longitudinal early diastolic LV basal myocardial velocities (7.4 cm/s vs. 6.8 cm/s; $p = 0.02$), although this reduction was more frequently observed in patients with idiopathic CP than those with secondary CP (7 of 7 [100%] vs. 7 of 12 [58%], respectively; $p = 0.06$).

Radial mechanics of LV. Peak radial strain of apical and mid LV segments was similar for all 3 groups, but peak radial strain of the LV base in CP was significantly reduced in comparison with control subjects and RCM ($p = 0.003$). Peak radial displacement correlated with peak circumferential shortening strains (Fig. 1) in CP, RCM, and control groups, and the association did not vary according to group status ($p = 0.51$). After pericardiectomy, radial strain was reduced significantly in the LV mid and basal regions ($26 \pm 11\%$ vs. $15 \pm 6\%$, $p = 0.001$, and $30 \pm 10\%$ vs. $20 \pm 14\%$, $p = 0.03$, respectively).

Circumferential LV mechanics and LV rotation. Peak circumferential shortening strains were significantly reduced in CP compared with both control subjects and RCM for all LV segments ($p \leq 0.001$) (Table 2). Peak LV rotation and rates of rotation during ejection, early diastole, and late diastole were similar in the 3 groups for the basal and mid segments (Table 3). However, in the LV apex, rotation and rates of rotation during ejection, early diastole, and late diastole were significantly reduced in CP compared with control subjects and RCM ($p < 0.001$ for both). Net LV twist, derived as the difference of apical and basal rotations, and indexed LV torsion (torsion normalized to LV length) were significantly lower in CP compared with RCM and control subjects ($p < 0.001$ for both). On combining the data from the 3 groups, peak global circumferential shortening strains correlated with the magnitude of net LV twist (Fig. 2). No differences were seen in circumferential deformation, LV rotation, net LV twist, and indexed LV torsion for idiopathic and secondary CP.

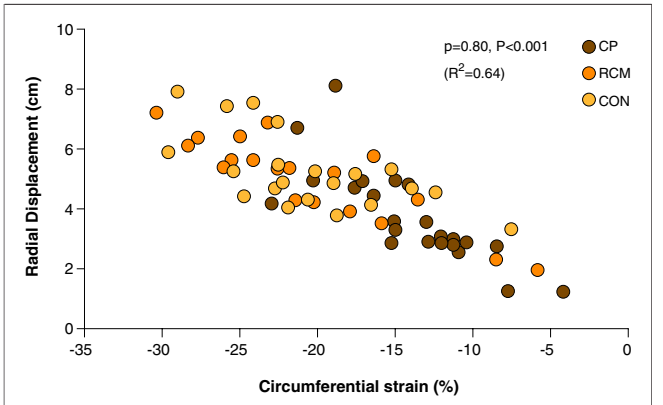

Figure 1. Relationship Between Left Ventricular Circumferential Strain and Radial Displacement

We used 2-dimensional speckle tracking echocardiography for determining circumferential strain **(x-axis)** and radial displacement **(y-axis)** in patients with constrictive pericarditis (CP), patients with restrictive cardiomyopathy (RCM), and control subjects (CON). Each plotted value represents peak end-systolic circumferential strain and radial displacement values averaged from apex, mid, and basal segments for 3 consecutive heartbeats. On combining the data from the 3 groups, peak radial displacement showed good correlation with peak circumferential shortening strains.

After pericardiectomy, circumferential strain, peak rotation, torsion, and rates of rotation or recoil at the LV apex, mid, and base remained unchanged (Table 4).

Table 3. Characterization of LV Rotational Mechanics

	Control Subjects (n = 21)	CP (n = 26)	RCM (n = 19)	p Value
Peak rotation,°				
Apex	19 (7)	6 (4)*†	18 (10)	<0.001
Mid	2 (5)	2 (4)	2 (7)	0.89
Base	5 (5)	−1 (4)	−4 (4)	0.09
Net twist,°	23 (7)	7 (5)*†	23 (10)	<0.001
Torsion (°/cm)	3 (1)	1 (1)*†	3 (1)	<0.001
Rotational rate,°/s				
Apex				
Peak S	108 (58)	37 (34)*†	122 (68)	<0.001
Peak E	116 (62)	−36 (50)*†	−122 (72)	<0.001
Peak A	−29 (35)	−13 (24)†	−69 (57)	<0.001
Mid				
Peak S	15 (58)	−3 (34)	18 (63)	0.69
Peak E	−13 (56)	1 (48)	−16 (66)	0.67
Peak A	2 (34)	9 (26)	−15 (64)	0.51
Base				
Peak S	−56 (41)	−33 (43)	−32 (36)	0.14
Peak E	54 (42)	30 (60)	31 (29)	0.24
Peak A	36 (30)	20 (23)	22 (27)	0.11

*CP versus control subjects, $p < 0.016$; †CP versus RCM, $p < 0.016$.
Abbreviations as in Table 2.

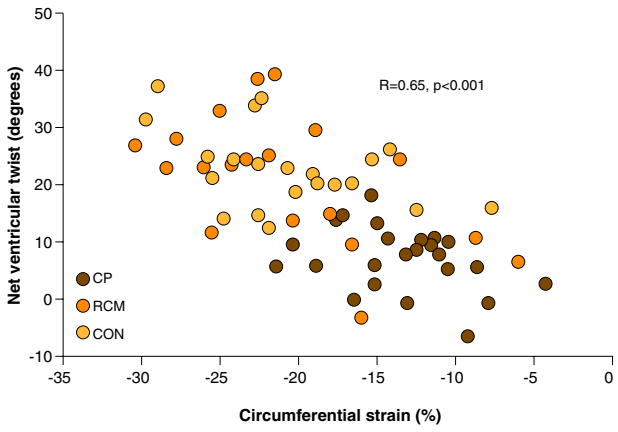

Figure 2. Relationship Between LV Circumferential Strain and Net Ventricular Twist

Peak end-systolic circumferential strain **(x-axis)** was averaged from basal, mid, and apical short-axis views for 3 consecutive heartbeats. Rotations in either the basal or apical short-axis planes were expressed as average angular displacements of 6 myocardial segments along the central axis. Net left ventricular (LV) twist **(y-axis)** was calculated as the net difference between LV peak rotation angles obtained from the basal and apical short-axis planes and averaged over 3 consecutive heartbeats. On combining the data from the 3 groups (CP, RCM, and CON), a good correlation was seen between peak circumferential shortening strains and peak net ventricular twist. Abbreviations as in Figure 1.

Longitudinal versus circumferential LV mechanics: diagnostic value. The distributions of various characteristics of LV mechanics among CP and RCM groups are displayed in Figure 3. For differentiating between CP and RCM, the area under the receiver-operating characteristic curve was significantly higher for early diastolic longitudinal velocities as compared with early diastolic untwisting velocities (0.97 vs. 0.76, respectively; p = 0.01) (Fig. 4). Figures 5 and 6 illustrate the differences in early diastolic LV recoil mechanics in CP and RCM by comparing early diastolic longitudinal velocity with early diastolic untwisting velocities.

Table 4. Change in LV Rotational Mechanics After Pericardiectomy

	CP Patients (n = 19)		p Value
	Pre-Operative	Post-Operative	
Peak rotation,°			
Apex	6 (4)	6 (1)	0.953
Mid	0.4 (5)	0 (5)	0.625
Base	−1 (5)	−2 (1)	0.781
Net twist,°	7 (6)	10 (7)	0.252
Torsion (°/cm)	1 (1)	2 (1)	0.274
Rotational rate,°/s			
Apex			
Peak S	41 (33)	39 (83)	0.622
Peak E	−35 (52)	−45 (75)	0.953
Peak A	−15 (24)	−6 (23)	0.65
Mid			
Peak S	−12 (39)	1 (54)	0.951
Peak E	17 (54)	12 (54)	0.79
Peak A	12 (26)	14 (31)	0.463
Base			
Peak S	−36 (43)	−51 (31)	0.926
Peak E	32 (60)	49 (21)	0.579
Peak A	24 (26)	33 (26)	0.179

Abbreviations as in Table 2.

DISCUSSION

To the best of our knowledge, this is the first study to provide simultaneous comparisons of the longitudinal, radial, and circumferential mechanics of the LV in CP and RCM. Whereas RCM was characterized by abnormal longitudinal LV mechanics with relative sparing of the LV rotation, patients with CP had relatively preserved longitudinal LV mechanics and a markedly abnormal circumferential deformation, torsion, and untwisting velocity.

Structural and functional anisotropy of transmural layers. Despite the right- and left-handed helical orientations of the subendocardial and subepicardial myofibers, both layers of the LV wall operate synergistically to create a functional continuum. Whereas the subendocardial region is responsible for longitudinal shortening, the subepicardial region causes LV circumferential shortening and torsion (1,15–17). Forces for longitudinal and circumferential deformation of LV arising at different transmural levels, however, act concurrently to shorten the subendocardial surface in 2 directions (1,15). Disease processes that predominantly affect the subendocardial fibers alter the longitudinal deformation of the LV wall. On the contrary, dysfunction of the outer subepicardial myofibers affects the circumferential deformation of the LV wall. In a normal human LV, the subendocardium shows higher strains in the circumferential direction, almost twice the magnitude of the longitudinal strain (18). Both components of LV mechanics can therefore be explored by tracking subendocardial deformation in the 2 orthogonal directions (13,14,19).

Disparate transmural mechanics in CP and RCM. We investigated LV mechanics in CP and RCM, 2 conditions in which LV early diastolic recoil is structurally constrained. In CP, the thickened, fused, and frequently calcified shell-like pericardial membranes tether the epimyocardial region. Furthermore, scarring, myocardial atrophy, and changes in collagen content are more pronounced over the

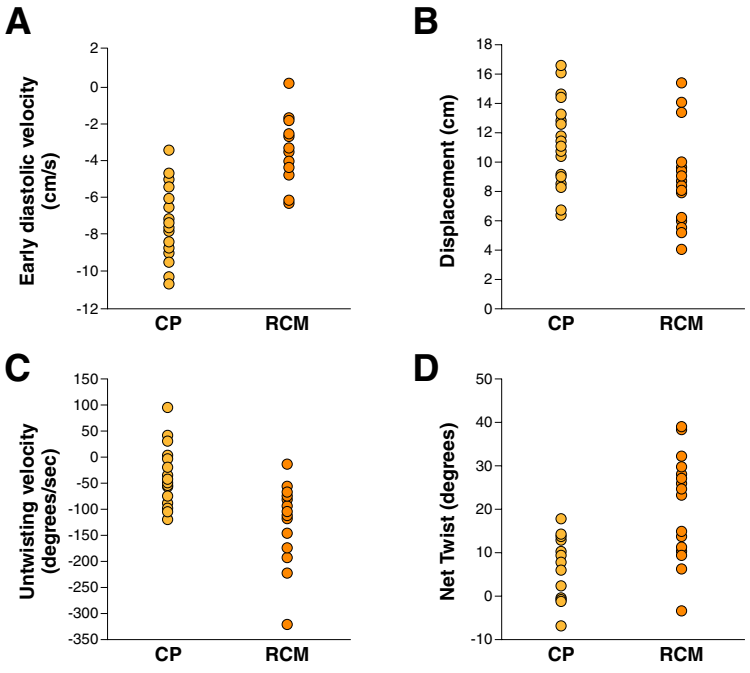

Figure 3. Longitudinal Versus Circumferential LV Mechanics

Distribution of peak early diastolic longitudinal velocity **(A)**, longitudinal displacement of the LV base **(B)**, peak early diastolic apical untwisting velocity **(C)**, and net ventricular twist **(D)** has been shown for patients with CP and RCM. In comparison with RCM, patients with CP had significantly higher longitudinal early diastolic velocity (E_m) and markedly attenuated untwisting velocity (E_r). Both velocities, when considered in isolation, however, show substantial overlap (E_m: 21 of 45 [47%]; longitudinal displacement: 36 of 45 [80%]; E_r: 23 of 45 [51%]; LV torsion: 24 of 45 [53%]). Abbreviations as in Figures 1 and 2.

epimyocardial region in CP (6–8). However, in RCM, infiltrative deposits and fibrosis predominate over the subendocardial region (20,21). In these 2 conditions, one would expect to find differentially altered patterns of LV circumferential and longitudinal mechanics.

Previous studies compared LV mechanics in CP and RCM with echo-Doppler methods, mostly relying on longitudinal motion data (5,22–25). We employed speckle tracking echocardiography, an angle-independent technique, which shows close correlation with measurements obtained via magnetic resonance imaging (9,19,26,27), and sonomicrometry (13, 14,19). We demonstrated that longitudinal displacement of the LV base was reduced in CP, consistent with previous observations (5), whereas longitudinal velocity and deformation were relatively spared. Interestingly, longitudinal strain values in CP were lower in the LV apical segments. The apex is the thinnest area of the LV where subendocardial and subepicardial myofibers show direct anatomical continuity (1). Tethering of the subepicardial region in CP might therefore influence longitudinal subendocardial deformation of the LV apex. In contrast, circumferential deformation in CP was markedly reduced for all

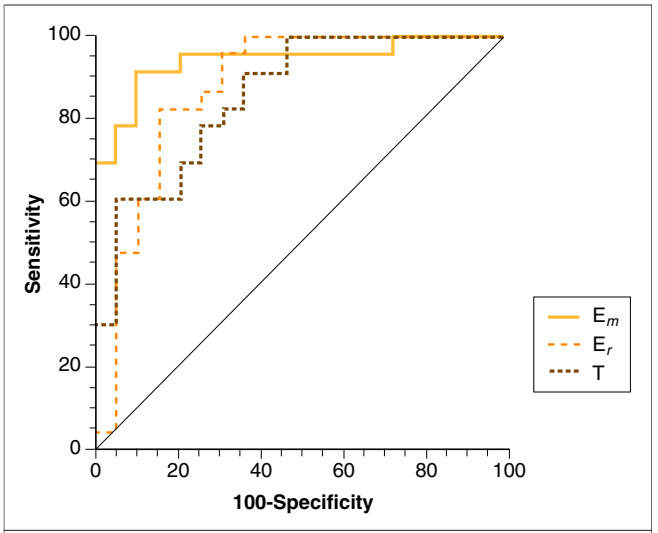

Figure 4. Receiver-Operating Characteristic Curve Analysis of Longitudinal and Torsional LV Mechanics

Receiver-operating characteristic curves of E_m, E_r, and net LV twist (T) have been plotted for differentiating CP from RCM. Optimal cut-off value for E_m was 5 cm/s (92% sensitivity and 90% specificity); E_r was −50°/s (57% sensitivity and 95% specificity); and net LV twist was 10° (83% sensitivity and 84% specificity). The area under the receiver-operating characteristic curve was significantly higher for early diastolic longitudinal velocities as compared with early diastolic untwisting velocities ($p = 0.01$). Abbreviations as in Figures 1 to 3.

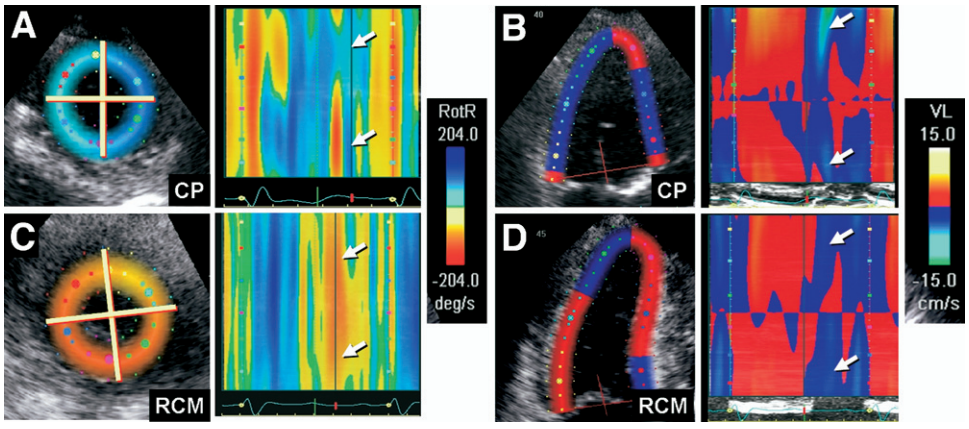

Figure 5. LV Longitudinal Velocity and Untwisting Velocity in CP and RCM

Color M-mode display of apical untwisting velocity (rotational rate of the LV apex [RotR]) obtained from speckle tracking of the LV apex in short-axis view shows markedly attenuated early diastolic rate of untwisting in CP **(A, arrows)**, whereas longitudinal early diastolic velocities (VL) from the LV base in apical 4-chamber view **(B, arrows)** are normal. In contrast, patients with RCM show a normal early diastolic rate of untwisting **(C, arrows)** and reduced longitudinal early diastolic velocities from the LV base **(D, arrows)**. Abbreviations as in Figures 1 and 2.

segments of the LV. This extends the observations of previous investigations in which circumferential shortening of the LV in CP was studied by cineangiographic techniques and reported to be significantly reduced (28–30).

In comparison with CP, patients with RCM showed relatively normal LV circumferential deformation and rotation and markedly reduced longitudinal velocities and deformation. This concurs with the observations of Henein and Gibson (21), who reported normal LV epicardial motion in RCM despite markedly reduced endocardial long-axis function. These findings are also consistent with observations in patients with myocardial diseases in whom abnormal long-axis function is accompanied with relatively spared LV torsion (10,11).

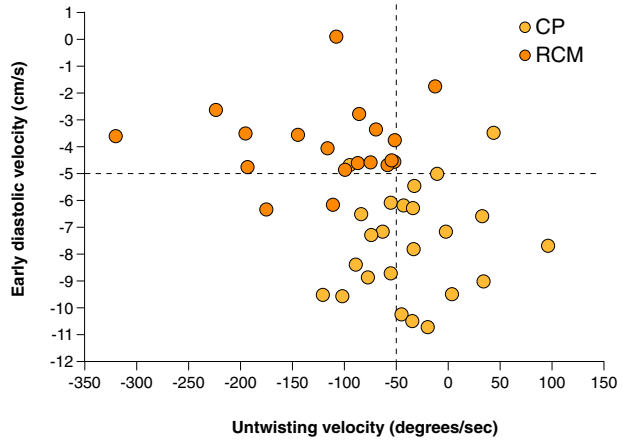

Figure 6. Comparison of Peak Longitudinal Early Diastolic Velocity With Peak Early Diastolic Untwisting Velocity

Early diastolic velocity >−5 cm/s and/or early diastolic apical untwisting velocity −50°/s separated the patients with CP and RCM with overlapping values seen in only 1 patient with CP. This finding provides a rationale for combining longitudinal early diastolic velocities with rotational untwisting velocities for differentiating the 2 disparate patterns of diastolic restoration mechanics seen in CP and RCM. Abbreviations as in Figure 1.

Radial deformation in CP was markedly attenuated at the LV base. Waters et al. (31) previously demonstrated a 5% end-systolic decrease in the volume enclosed by the pericardial sack in healthy hearts, primarily manifesting as a radial diminution of the pericardial/epicardial contour of the LV. Emilsson et al. (32) further showed that the radial movement of epicardial surface of the LV was greatest at the base and lowest at the mid level. Tethering of the epicardial surface in CP might therefore limit the radial motion of myocardial segments, particularly near the LV base.

CP: a heterogenous disease. Constrictive pericarditis in the modern era is a heterogeneous disease (33,34). A substantial number of patients with secondary CP (previous cardiac surgery, radiation) have low longitudinal early diastolic velocities and show regional heterogeneity in LV mechanics (24,25,35–37). To circumvent this limitation, we averaged 2D strain parameters from 6 segments in short-axis views and from lateral and septal wall segments in apical 4-chamber views. Deformation measured by speckle tracking, when averaged from multiple locations, provides a robust measure of global LV diastolic function (38). On comparing the averaged early diastolic longitudinal and untwisting velocities, the overlap between CP and RCM was substantially reduced. This

finding provides a rationale for combining longitudinal early diastolic velocities with untwisting velocities for improved clinical differentiation of CP from RCM and requires confirmation in further studies.

Effects of pericardiectomy. Immediately after pericardiectomy, a reduction in early diastolic mitral annular velocity was observed in a majority of patients, although LV rotation and untwisting velocities remained unchanged. This suggests that pericardiectomy might not immediately normalize LV mechanics in patients with CP. Indeed, previous studies have shown that after pericardiectomy, although symptoms of heart failure improve, the majority of patients have persistent signs of constriction on echocardiography (39). Vogel et al. (30) have also found that LV circumferential shortening and velocity remain persistently abnormal after pericardiectomy. Pericardiectomy might not restore a frictionless surface that is required for normal cardiac rotation. Furthermore, because the epicardial dysfunction and fibrosis might be chronic, an immediate post-operative recovery of LV function might not be evident. Studies with a longer duration of follow-up will be required to explore these possibilities.

Study limitations. The application of speckle tracking depends on the resolution of 2D image, and this might be suboptimal in CP. Furthermore, for the calculation of LV rotation, the exact location of the basal and apical plane might vary from patient to patient and might induce measurement error. In the present study we attempted to reduce this error by measuring apical twist at a location as close to the LV apex as possible, preferably where the right ventricular cavity was no longer visible in the cross-sectional plane. Cardiac catheterization data were not available for all RCM patients, primarily because catheterization was not clinically indicated. However, the presence of severe left atrial enlargement in this group provided indirect evidence of chronically elevated LV filling pressures (40). Recruitment of control subjects who were younger than CP patients would be likely to attenuate real differences in LV circumferential deformation between groups, because it has been previously shown that LV torsion increases with age (41,42). Accordingly, the decrease in LV torsion in CP should be even more noticeable when compared with age-matched control subjects. Further studies are warranted to confirm this assertion.

CONCLUSIONS

This study confirms the hypothesis that patients with CP have impaired LV circumferential deformation, torsion, and subsequent recoil in early diastole. Assessment of variations in longitudinal and circumferential LV recoil mechanics by 2D speckle tracking differentiates the 2 distinct patterns of diastolic restoration mechanics seen in CP and RCM.

Reprint requests and correspondence: Dr. Bijoy K. Khandheria, Division of Cardiovascular Diseases, Mayo Clinic, 13400 East Shea Boulevard, Scottsdale, Arizona 85259. *E-mail: khandheria@mayo.edu.*

REFERENCES

1. Sengupta PP, Korinek J, Belohlavek M, et al. Left ventricular structure and function: basic science for cardiac imaging. J Am Coll Cardiol 2006;48:1988–2001.
2. Notomi Y, Martin-Miklovic MG, Oryszak SJ, et al. Enhanced ventricular untwisting during exercise: a mechanistic manifestation of elastic recoil described by Doppler tissue imaging. Circulation 2006;113:2524–33.
3. Gibbons Kroeker CA, Adeeb S, Tyberg JV, Shrive NG. A 2D FE model of the heart demonstrates the role of the pericardium in ventricular deformation. Am J Physiol Heart Circ Physiol 2006;291:H2229–36.
4. Lee JM, Boughner DR. Tissue mechanics of canine pericardium in different test environments. Evidence for time-dependent accommodation, absence of plasticity, and new roles for collagen and elastin. Circ Res 1981;49:533–44.
5. Garcia MJ, Rodriguez L, Ares M, Griffin BP, Thomas JD, Klein AL. Differentiation of constrictive pericarditis from restrictive cardiomyopathy: assessment of left ventricular diastolic velocities in longitudinal axis by Doppler tissue imaging. J Am Coll Cardiol 1996;27:108–14.
6. Levine HD. Myocardial fibrosis in constrictive pericarditis. Electrocardiographic and pathologic observations. Circulation 1973;48:1268–81.
7. Chello M, Mastroroberto P, Romano R, Perticone F, Marchese AR. Collagen network remodelling and left ventricular function in constrictive pericarditis. Heart 1996;75:184–9.
8. Dave T, Narula JP, Chopra P. Myocardial and endocardial involvement in tuberculous constrictive pericarditis: difficulty in biopsy distinction from endomyocardial fibrosis as a cause of restrictive heart disease. Int J Cardiol 1990;28:245–51.
9. Notomi Y, Lysyansky P, Setser RM, et al. Measurement of ventricular torsion by two-dimensional ultrasound speckle tracking imaging. J Am Coll Cardiol 2005;45:2034–41.
10. Chung J, Abraszewski P, Yu X, et al. Paradoxical increase in ventricular torsion and systolic torsion rate in type I diabetic patients under tight glycemic control. J Am Coll Cardiol 2006;47:384–90.
11. Young AA, Kramer CM, Ferrari VA, Axel L, Reichek N. Three-dimensional left ventricular deformation in hypertrophic cardiomyopathy. Circulation 1994;90:854–67.
12. Gottdiener JS, Bednarz J, Devereux R, et al. American Society of Echocardiography recommendations for use of echocardiography in clinical trials. J Am Soc Echocardiogr 2004;17:1086–119.

13. Korinek J, Wang J, Sengupta PP, et al. Two-dimensional strain—a Doppler-independent ultrasound method for quantitation of regional deformation: validation in vitro and in vivo. J Am Soc Echocardiogr 2005; 18:1247–53.
14. Korinek J, Kjaergaard J, Sengupta PP, et al. High spatial resolution speckle tracking improves accuracy of 2-dimensional strain measurements: an update on a new method in functional echocardiography. J Am Soc Echocardiogr 2007;20:165–70.
15. Sengupta PP, Khandheria BK, Korinek J, et al. Apex-to-base dispersion in regional timing of left ventricular shortening and lengthening. J Am Coll Cardiol 2006;47:163–72.
16. Taber LA, Yang M, Podszus WW. Mechanics of ventricular torsion. J Biomech 1996;29:745–52.
17. Davis JS, Hassanzadeh S, Winitsky S, et al. The overall pattern of cardiac contraction depends on a spatial gradient of myosin regulatory light chain phosphorylation. Cell 2001; 107:631–41.
18. Bogaert J, Rademakers FE. Regional nonuniformity of normal adult human left ventricle. Am J Physiol Heart Circ Physiol 2001;280:H610–20.
19. Helle-Valle T, Crosby J, Edvardsen T, et al. New noninvasive method for assessment of left ventricular rotation: speckle tracking echocardiography. Circulation 2005;112:3149–56.
20. Maceira AM, Joshi J, Prasad SK, et al. Cardiovascular magnetic resonance in cardiac amyloidosis. Circulation 2005; 111:186–93.
21. Henein MY, Gibson DG. Abnormal subendocardial function in restrictive left ventricular disease. Br Heart J 1994;72:237–42.
22. Ha JW, Oh JK, Ommen SR, Ling LH, Tajik AJ. Diagnostic value of mitral annular velocity for constrictive pericarditis in the absence of respiratory variation in mitral inflow velocity. J Am Soc Echocardiogr 2002;15: 1468–71.
23. Ha JW, Ommen SR, Tajik AJ, et al. Differentiation of constrictive pericarditis from restrictive cardiomyopathy using mitral annular velocity by tissue Doppler echocardiography. Am J Cardiol 2004;94:316–9.
24. Sengupta PP, Mohan JC, Mehta V, Arora R, Pandian NG, Khandheria BK. Accuracy and pitfalls of early diastolic motion of the mitral annulus for diagnosing constrictive pericarditis by tissue Doppler imaging. Am J Cardiol 2004;93:886–90.
25. Rajagopalan N, Garcia MJ, Rodriguez L, et al. Comparison of new Doppler echocardiographic methods to differentiate constrictive pericardial heart disease and restrictive cardiomyopathy. Am J Cardiol 2001;87:86–94.
26. Li Y, Garson CD, Xu Y, et al. Quantification and MRI validation of regional contractile dysfunction in mice post myocardial infarction using high resolution ultrasound. Ultrasound Med Biol 2007;33:894–904.
27. Cho GY, Chan J, Leano R, Strudwick M, Marwick TH. Comparison of two-dimensional speckle and tissue velocity based strain and validation with harmonic phase magnetic resonance imaging. Am J Cardiol 2006; 97:1661–6.
28. Sekino E, Suzuki S, Momokawa T, Kudo T, Ihaya A, Ishizuka N. Left ventricular function studies in constrictive pericarditis. Jpn J Surg 1978; 8:186–91.
29. Shabetai R. Left ventricular function and myocardial contractility in chronic constrictive pericarditis. Chest 1971; 59:476–7.
30. Vogel JH, Horgan JA, Strahl CL. Left ventricular dysfunction in chronic constrictive pericarditis. Chest 1971; 59:484–92.
31. Waters EA, Bowman AW, Kovacs SJ. MRI-determined left ventricular "crescent effect": a consequence of the slight deviation of contents of the pericardial sack from the constant-volume state. Am J Physiol Heart Circ Physiol 2005; 288:H848–53.
32. Emilsson K, Kahari A, Bodin L, Thunberg P. Outer contour and radial changes of the cardiac left ventricle: a magnetic resonance imaging study. Clin Res Cardiol 2007;96:272–8.
33. Ling LH, Oh JK, Schaff HV, et al. Constrictive pericarditis in the modern era: evolving clinical spectrum and impact on outcome after pericardiectomy. Circulation 1999;100:1380–6.
34. Babuin L, Alegria JR, Oh JK, Nishimura RA, Jaffe AS. Brain natriuretic peptide levels in constrictive pericarditis and restrictive cardiomyopathy. J Am Coll Cardiol 2006;47:1489–91.
35. Choi EY, Ha JW, Kim JM, et al. Incremental value of combining systolic mitral annular velocity and time difference between mitral inflow and diastolic mitral annular velocity to early diastolic annular velocity for differentiating constrictive pericarditis from restrictive cardiomyopathy. J Am Soc Echocardiogr 2007;20:738–43.
36. Butz T, Langer C, Scholtz W, et al. Severe calcification of the lateral mitral annulus in constrictive pericarditis: a potential pitfall for the use of echocardiographic tissue Doppler imaging. Eur J Echocardiogr 2007. In press.
37. Arnold MF, Voigt JU, Kukulski T, Wranne B, Sutherland GR, Hatle L. Does atrioventricular ring motion always distinguish constriction from restriction? A Doppler myocardial imaging study. J Am Soc Echocardiogr 2001;14:391–5.
38. Wang J, Khoury DS, Thohan V, Torre-Amione G, Nagueh SF. Global diastolic strain rate for the assessment of left ventricular relaxation and filling pressures. Circulation 2007;115: 1376–83.
39. Senni M, Redfield MM, Ling LH, Danielson GK, Tajik AJ, Oh JK. Left ventricular systolic and diastolic function after pericardiectomy in patients with constrictive pericarditis: Doppler echocardiographic findings and correlation with clinical status. J Am Coll Cardiol 1999;33:1182–8.
40. Abhayaratna WP, Seward JB, Appleton CP, et al. Left atrial size: physiologic determinants and clinical applications. J Am Coll Cardiol 2006;47: 2357–63.
41. Nakai H, Takeuchi M, Nishikage T, Kokumai M, Otani S, Lang RM. Effect of aging on twist-displacement loop by 2-dimensional speckle tracking imaging. J Am Soc Echocardiogr 2006;19:880–5.
42. Notomi Y, Srinath G, Shiota T, et al. Maturational and adaptive modulation of left ventricular torsional biomechanics: Doppler tissue imaging observation from infancy to adulthood. Circulation 2006;113:2534–41.